NAVAL POSTGRADUATE SCHOOL

MONTEREY, CALIFORNIA

THESIS

TRACKING THE MORPHOLOGICAL CHANGES DURING A DRY VERSUS RAINY SEASON AT THE PAJARO RIVER ESTUARY USING UAS

by

Joshua J. Helms

December 2023

Thesis Advisor: Mara S. Orescanin
Second Reader: Larry Gulliver, Naval Research Laboratory

THIS PAGE INTENTIONALLY LEFT BLANK

REPORT DOCUMENTATION PAGE	*Form Approved OMB No. 0704-0188*

1. AGENCY USE ONLY *(Leave blank)*	**2. REPORT DATE** December 2023	**3. REPORT TYPE AND DATES COVERED** Master's thesis

4. TITLE AND SUBTITLE TRACKING THE MORPHOLOGICAL CHANGES DURING A DRY VERSUS RAINY SEASON AT THE PAJARO RIVER ESTUARY USING UAS	**5. FUNDING NUMBERS**
6. AUTHOR(S) Joshua J. Helms	
7. PERFORMING ORGANIZATION NAME(S) AND ADDRESS(ES) Naval Postgraduate School Monterey, CA 93943-5000	**8. PERFORMING ORGANIZATION REPORT NUMBER**
9. SPONSORING / MONITORING AGENCY NAME(S) AND ADDRESS(ES) N/A	**10. SPONSORING / MONITORING AGENCY REPORT NUMBER**

11. SUPPLEMENTARY NOTES The views expressed in this thesis are those of the author and do not reflect the official policy or position of the Department of Defense or the U.S. Government.

12a. DISTRIBUTION / AVAILABILITY STATEMENT Approved for public release. Distribution is unlimited.	**12b. DISTRIBUTION CODE** A

13. ABSTRACT (maximum 200 words)

Drastic morphological change occurs annually at the ephemeral river at Pajaro River beach as an inlet is created upon breaching to the Monterey Bay. This inlet breach, and subsequent migration of that inlet, affects the local community with increased flood events and ecological impacts with loss of access to the bay, and it can be hazardous for Amphibious and Naval Special Warfare (NSW) operations at similar beach sites. River discharge, river height, significant wave height, and wave radiation stress all contribute inlet breaching and subsequent migration. Once breached, the inlet at Pajaro migrates south before ultimately closing toward the end of the water year. Using unmanned aerial systems (UAS) with a LiDAR payload, UAS for videography and photography, GNSS walking surveys, and Sentinel L-2A satellite data, this study collected two water years of data (01OCT2021–30SEP2023) to compare a heavy precipitation water year (2023) to a normal, or dry, water year (2022), to better understand inlet breaching, closure, and migration rates. This study shows that during wetter winter months, inlet migration is dominated by high river discharge from the increased amount of rain water. Once the transition to summer occurs, the dominant factor in inlet migration is offshore waves. For a high precipitation water year, this study shows the inlet migration travels farther, the inlet stays open longer than the typical annual cycle, and fewer (zero for this case) closures will occur.

14. SUBJECT TERMS ephemeral river, unmanned systems, UAS, aerial photography, inlet migration, beach morphology, LiDAR, nearshore sediment transport, river discharge, Pajaro River, topography, wave height	**15. NUMBER OF PAGES** 69
	16. PRICE CODE

17. SECURITY CLASSIFICATION OF REPORT	**18. SECURITY CLASSIFICATION OF THIS PAGE**	**19. SECURITY CLASSIFICATION OF ABSTRACT**	**20. LIMITATION OF ABSTRACT**
Unclassified	Unclassified	Unclassified	UU

NSN 7540-01-280-5500

Standard Form 298 (Rev. 2-89)
Prescribed by ANSI Std. 239-18

THIS PAGE INTENTIONALLY LEFT BLANK

Approved for public release. Distribution is unlimited.

TRACKING THE MORPHOLOGICAL CHANGES DURING A DRY VERSUS RAINY SEASON AT THE PAJARO RIVER ESTUARY USING UAS

Joshua J. Helms
Lieutenant Commander, United States Navy
BS, United States Naval Academy, 2011

Submitted in partial fulfillment of the
requirements for the degree of

MASTER OF SCIENCE IN METEOROLOGY AND PHYSICAL OCEANOGRAPHY

from the

NAVAL POSTGRADUATE SCHOOL
December 2023

Approved by: Mara S. Orescanin
Advisor

Larry Gulliver
Second Reader

Peter C. Chu
Chair, Department of Oceanography

THIS PAGE INTENTIONALLY LEFT BLANK

ABSTRACT

Drastic morphological change occurs annually at the ephemeral river at Pajaro River beach as an inlet is created upon breaching to the Monterey Bay. This inlet breach, and subsequent migration of that inlet, affects the local community with increased flood events and ecological impacts with loss of access to the bay, and it can be hazardous for Amphibious and Naval Special Warfare (NSW) operations at similar beach sites. River discharge, river height, significant wave height, and wave radiation stress all contribute inlet breaching and subsequent migration. Once breached, the inlet at Pajaro migrates south before ultimately closing toward the end of the water year. Using unmanned aerial systems (UAS) with a LiDAR payload, UAS for videography and photography, GNSS walking surveys, and Sentinel L-2A satellite data, this study collected two water years of data (01OCT2021–30SEP2023) to compare a heavy precipitation water year (2023) to a normal, or dry, water year (2022), to better understand inlet breaching, closure, and migration rates. This study shows that during wetter winter months, inlet migration is dominated by high river discharge from the increased amount of rain water. Once the transition to summer occurs, the dominant factor in inlet migration is offshore waves. For a high precipitation water year, this study shows the inlet migration travels farther, the inlet stays open longer than the typical annual cycle, and fewer (zero for this case) closures will occur.

THIS PAGE INTENTIONALLY LEFT BLANK

TABLE OF CONTENTS

LIST OF FIGURES

LIST OF ACRONYMS AND ABBREVIATIONS

BBE	Bar-Built Estuary
CDIP	Coastal Data Information Program
CiRN	Coastal Imaging Research Network
CNMOC	Naval Meteorology and Oceanography Command
CNO	Chief of Naval Operations
CORS	Continuously Operating Reference Station
DME	Distributed Maritime Environment
d_r	River Discharge Rate
ENSO	El Nino-Southern Oscillation
FoV	Field of View
GCP	Ground Control Point
GNSS	Global Navigation Satellite System
GPS	Global Positioning System
h_r	River Height
Hs	Significant Wave Height
ICOLL	Intermittent Closed/Open Lakes & Lagoons
LiDAR	Light Detection and Ranging
METOC	Meteorology and Oceanography
NOAA	National Oceanic and Atmospheric Administration
NSW	Naval Special Warfare
PaRS	Photogrammetry and Remote Sensing
Q_m	Max flow Rate per Second during Tidal Cycle
QT Modeler	Quick Terrain Modeler
SMS	Aquaveo Surface-Water Measuring Software
SWAN	Simulated Waves Nearshore
S_{xx}	On Shore Wave Radiation Stress
S_{xy}	Along-shore Wave Radiation Stress

TOCE	Temporary Open/Closed Estuary
UAV	Unmanned Aerial Vehicle
USGS	United States Geological Survey
USV	Unmanned Surface Vehicle
UUV	Unmanned Underwater Vehicle
UxS	Unmanned Systems
WY	Water Year
Θ	Wave Direction

ACKNOWLEDGMENTS

Thank you very much to Dr. Mara Orescanin for taking me on as a thesis student considering she had four other students at the time. I know I originally came along to play with her expensive toys and play on the beach. However, I know that I would not have finished this thesis under the guidance of another advisor. Her energy, passion, and positive attitude toward everything made this difficult journey enjoyable!

To my second reader, Dr. Larry Gulliver, where would I be without your help? The answer is: much further behind! Instead, your wisdom, guidance, mentorship, and patience allowed me to be ahead of the game the whole way through. You embody the definition of an Officer and a Gentleman. I have learned a lot from you, and I hope to emulate your outstanding qualities as I continue my Naval career. Thank you, my friend.

To the Bob Ross of MATLAB (Mike Cook), I cannot thank you enough. There is absolutely no way I finish this project without your hours of help.

Paul Jessen, thank you for the days and days of field work help.

To Maj. Justin Crisp, USMC, thank you my brother. I am so glad I had the privilege of working with you. You are a true professional, and I'm excited that you get to teach at the finest institution in the world: USNA.

To my cohort, thanks to each and every one of you. I have greatly enjoyed our 2.5 years together, and I looked forward to seeing everyone out in the Fleet!

Finally, I would like to thank my wife, Brittany. Through all the days I thought I wouldn't make it; you were always there pushing me through. It only took 10 years, but I finally got you to California! Now, let's get back to Virginia!

THIS PAGE INTENTIONALLY LEFT BLANK

I. MOTIVATION

The U.S. Navy has, and will continue to have, a strong interest in the environmental factors surrounding coastal and littoral regions. On the operation side, amphibious landings are a critical mission set for NSW personnel as well as the Marines. A thorough understanding of beach landing zones and their continuously evolving environment are paramount for successful amphibious operations anywhere on the globe. For Naval engineering, beach morphologic changes, wave run up, and sediment build up/erosion are key factors for deciding where to build new facilities. Naval engineers need to have constant updates and awareness on these factors that can affect shores and coastlines for planning naval infrastructures.

One answer to this is the use of Unmanned Systems (UxS). In recent years, their use in the Navy has seen a drastic increase with no signs of slowing. The Department of the Navy (DON) released the Unmanned Campaign Framework in 2021 in order to put a focus on the constantly expanding UxS presence in our nation's military. The Chief of Naval Operations (CNO) ADM M.M. Gilday predicts UAVs, UUVs, and USVs will have key roles in a Distributed Maritime Environment (DME) in the future. Consequently, Commander Naval Meteorology and Oceanography Command (CNMOC) has obtained a vast arsenal of UUV's of all shapes, sizes, capabilities, that are equipped for various mission sets. CNMOC's UUVs, along with the personnel, operate all over the world conducting support operations for all branches of the military and in support of our allies. The military personnel who operate these unmanned systems undergo months of extensive training to earn the qualifications required to safely use them. As of today, the Department of the Navy (DON) does not have an enlisted rating specifically for UUV operations. This means personnel who get stationed to these unmanned specific commands, gain these valuable skills, and rotate (receive orders to be stationed elsewhere) out with that knowledge that may never be used again at follow on commands. This costs the DON a lot of money and time having to train new personnel every time people transition.

Unlike UUV's, unmanned aerial systems (UAS) are not as prolifically used in the Meteorology and Oceanography (METOC) community with the exception being the NSW

community where they are used and relied on heavily. The Navy in general is slowly ramping up the use of UAS, but. Likely reasons for this are that UAS are historically expensive, require extensive training, had low payload capacity, limited endurance, and limited capability. However, all of these negative aspects are quickly becoming a thing of the past. UAS drones are now very inexpensive with very capable systems ranging anywhere from a few hundred to a few thousand dollars. Additionally, the training required, although still extensive, is more streamlined and user interfaces have been greatly enhanced from previous years. Current Navy oceanographic research requirements and/or problem sets (i.e., sediment migration, beach morphologic changes, and nearshore analysis) can be effectively and efficiently tackled with the use of UAS systems to greatly enhance future operations and support.

II. INTRODUCTION

A. BACKGROUND

A bar-built estuary (BBE), also known as a temporary open/closed estuary (TOCE), and intermittent closed/open lakes and lagoons (ICOLLs) and/or ephemeral rivers, are all terms for river mouths that flow for short periods from river discharge from heavy rainfall or snowmelt upstream (Booysen and Theron 2020; McSweeney et al. 2017). Ephemeral rivers are rivers that flow after heavy precipitation and/or snow melt. They can be classified as either being regular (seasonal breaching and closure) or irregular (a less predictable cycle) (Davidson et al. 2009). The Earth has over 1,400 ephemeral rivers on six continents, as seen by the black dots in Figure 1 (McSweeney et al. 2017). ICOLLs make up 3 percent of all ephemeral rivers, with 15% of those being defined as microtidal ephemeral rivers (McSweeney et al. 2017).

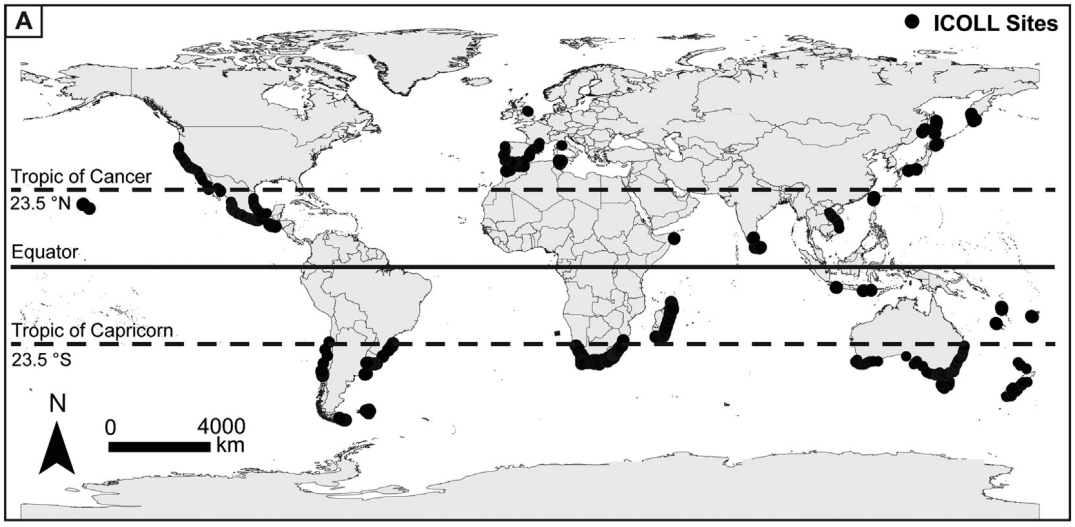

Figure 1. ICOLLs located across the globe. Source: McSweeney et al. (2017).

Several studies have shown that prolonged beach closures can have detrimental effects on the local community and ecosystem such as flooding upstream, large variations in lagoon salinity, decrease in lagoon water quality, and prevention of fish migration from

lagoon to bay (Kraus et al. 2002; Davidson et al. 2009; Orescanin and Scooler 2018). Water quality (dissolved oxygen) is often highly variable, both spatially and temporally, as a result of variable estuarine flushing depending on the inlet width. (Dawson et al. 2023). Additionally, the migration pattern of the inlet mouth is not always static meaning that in some locations the inlet will migrate in one direction or the other before a closure event (Orescanin et al. 2019). The depth of the inlet and the surrounding currents can play a role in the stability of inlet migration (Fitzgerald et al. 1978; Tung et al. 2009).

Breaching events occur when enough river discharge is present to break through the sand barrier out to the sea. Breaching can have positive and negative consequences (Kraus et al. 2008). A breach reduces flooding risks for communities just upstream by lowering the water level in the river and its associated lagoon, as well as providing a path for fish to return to the sea, sometimes improving water quality through estuarine flushing. The negative aspects come from the "urban drool" and agricultural runoff that have been trapped in the lagoon. These pollutants can lower the water quality and negatively impact the local ecosystem. From ecosystem disruptions, water quality, fishing implications, flooding risks, and military amphibious/beach operations, these rivers and beaches can cause not only significant impacts to the local communities around them, but also to naval operations.

B. BREACHING/CLOSURE ECONOMIC AND NAVAL IMPACTS

Breaching of an ephemeral river can cause loss of life, property loss/damage, changes in water level and salinity, endanger wildlife, and disrupt operations (Kraus et al. 2002; Wainwright and Baldock 2015; Booysen and Theron 2020; Orescanin et al. 2021). On the other side, prolonged closure can cause flooding for surrounding communities, negatively impact the chemical properties of the estuary, and disrupt local ecosystems (Booysen and Theron 2020; Whitfield et al. 2012). As such, quantifying the effects of mouth state on lagoon water levels (and consequently upstream water levels), both natural and artificial, coupled with frequent monitoring of the breach will help save lives, property, crops, and the local ecosystem. Being able to predict inlet breach openings, closures, and

inlet migration patterns of the Pajaro River could help reduce government waste and, more importantly, help prepare and protect the local community.

The Navy and Marine Corps. implications of breaching are vast. Amphibious operation planning and execution become increasingly more difficult due to the uncertainty of magnitude and longevity of these breaches. UxS operations are conducted from beaches all over the world. Conducting one of these missions during an unplanned active breach could lead to mission failure, loss of equipment, or even loss of life. Additionally, military installation planning and management agencies, such as the Army Corps of Engineers, can benefit greatly from breaching data when it comes to constructing buildings and predicting the impact to them on ephemeral beaches (Douglass 1992). For the Navy and Marine Corps. to be successful, understanding the dynamic nature of these beaches is paramount. Following a closure, variations to beach slope and stability can affect amphibious landing operations if not properly accounted for.

C. UAS REMOTE SENSING FOR BEACH ANALYSIS (WHAT HAS BEEN DONE)

Traditional methods over the last few decades of tracking beach morphological change are comprised of either running models and/or taking physical ground measurements on site (Ranasinghe and Pattiaratchi 2003; Tung et al. 2009; Rich and Keller 2013). Model runs, both analytic and numeric, provide a general representation of what could happen under static, or 'normal', conditions. However, uncertainty in model predictions for ephemeral river breaching and closure can lead to the inability to accurately forecast the beach's morphological evolution. Using UAS for scientific research, specifically for Photogrammetry and Remote Sensing (PaRS), has only been conducted in the last couple of decades (Holland et al. 1995; Colomina and Molina 2014; Casella et al. 2020). For studying ephemeral rivers and beach environments, the art of using UAS is even more recent (Casella et al. 2020; Orescanin et al. 2021, 2019).

Unmanned aerial systems are new assets for conducting beach migration research, and completely change the way, speed, and efficiency in which data is collected. UAS data collection has advantages over the traditional ground measurements, which may provide

ground truth but are extensively more costly with regard to time and human resources while providing less spatial coverage. Aerial systems provide a full picture view of the research area, which would otherwise require a high vantage point either from an airplane, cliff, nearshore structure, or satellite image that lacks sufficient horizontal resolution. Additionally, the overall cost of highly capable systems has drastically reduced over the years making these systems more affordable. They provide high resolution data quickly and require a reduced footprint. Because of this, we have seen a substantial increase of beach environment research using UAS in the last few years (Casella et al. 2020).

D. TIDAL INLET MIGRATION

Like tidal inlets that also create vast changes of the beach morphology, predicting tidal inlet rate and direction of migration of ephemeral rivers is a difficult task. However, looking at tidal inlet migration first may give some hints as to why ephemeral rivers behave the way they do.

Several studies calculate sediment transport direction and magnitudes that are directly related to tidal inlet migration (Bruun 1960; Ranasinghe and Pattiaratchi 2003; Tung et al. 2009; Davidson et al. 2009). Bruun 1960 concluded that Q_m (maximum flow rate per second of the tidal cycle) was a superior parameter than the tidal prism to determine the characterizations of the inlet as it is directly related to bottom shear stress, τ (Bruun, 1960). Other studies built on Bruun's work determined that inlet sedimentation infilling and backfilling are key factors in sediment transportation, and ultimately, inlet closure (Ranasinghe and Pattiaratchi 2003; Tung et al. 2009; Davidson et al. 2009). Migration of tidal inlets depends on many factors ranging from ebb tidal current velocity (determined by the tidal prism and inlet cross-sectional area), river/ocean/bay currents, the magnitude of littoral drift, composition of the beach/channel, and depth of the channel inlet (Fitzgerald 1988). In addition to the Fitzgerald findings, Aubrey and Speer (1984) discovered three mechanisms responsible for the updrift migration of tidal inlets (or inlets that migrate opposite of the net longshore transport); the inclusion of tidal deltas to the barrier spit, heavy precipitation induced breaching followed by stabilization of a new inlet location,

and ebb tidal discharge around the breach opening in which the current pattern erodes the channel and deposits the sediment on the inner channel bank (Aubrey & Speer, 1984).

In contrast to tidal inlets, there has been significantly less research regarding migration of inlets at small river mouths. Behrens et al. had a 33 year study looking at the migration patterns of the Russian River estuary in California to better understand the morphological changes over the course of varying ENSO (El Nino-Southern Oscillation) cycles (Behrens et al. 2009). Total annual migration on the order of 250 m for wet months and 100 m for dry months occurred at this site, with no preferential direction, though this was thought to be ENSO related. For inlet migration, they concluded that during periods of high river discharge that the inlet had increased migration distances and rates, but during dryer low river discharge periods that waves played the dominant role in morphologic change (Behrens et al. 2009). For the Russian River they found that H_s gradients of at least 0.5 m/day or greater lead to inlet migration, and that river discharge rates of 80 $m\text{^}3/s$ or greater lead to 45 percent of inlet migration rates of 15 m/day (Behrens et al. 2009).

These works laid the foundation for understanding how inlet migrations work. However, with the exception of Behrens work in 2009, little research has been done on predicting inlet migration rates and distances for BBEs where intermittent discharge and breaching/closure affect morphodynamics. Additionally, little has been done to discover where the system transitions from purely tidally driven to riverine depending on river discharge, tidal waves, and seasonal precipitation amounts. Arguably, the migration of ephemeral rivers is an even more complex problem since they typically shift only while the breach is open as seen in Figure 2. Since there are few studies that quantify rates of migration for these abnormal rivers, the forcing behind their movement is not well understood.

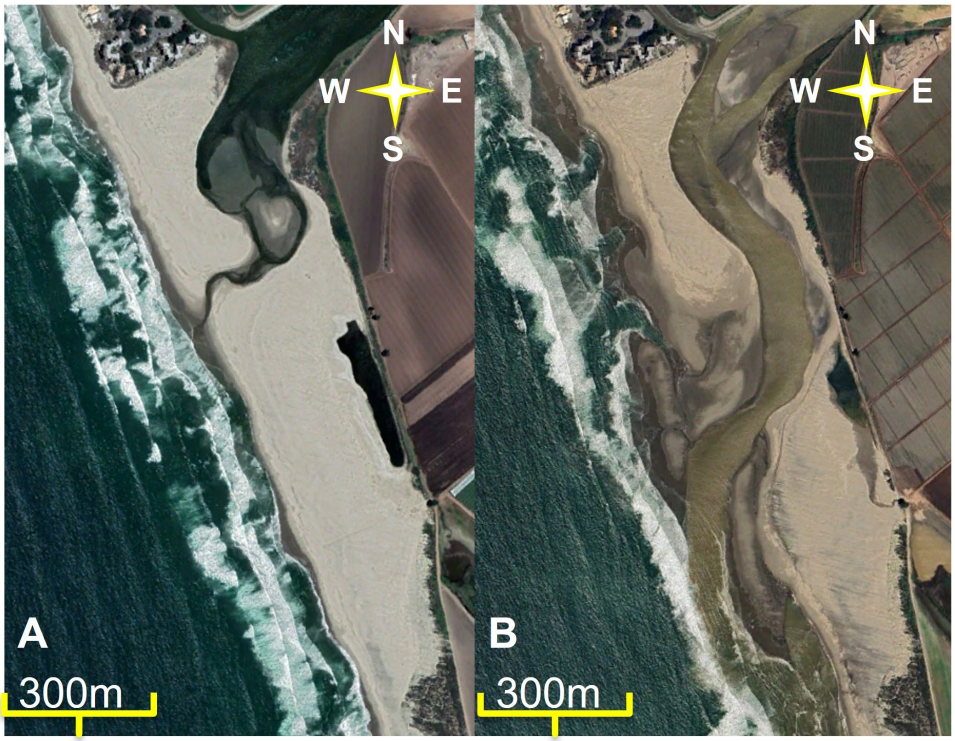

Figure 2. Satellite imagery of Pajaro River breach June 2022 (a) and April 2023 (b). Adapted from Google Earth (2023).

E. PAJARO RIVER BEACH OVERVIEW

The Pajaro River was chosen as it is an ephemeral river along the California coast that is known to migrate between periods of closure, as seen in Figure 2. The Pajaro River beach is located approximately ten miles north of Monterey and situated centrally along the coastline of Monterey Bay. The beach is approximately 1,300 meters in length from the start of the Pajaro Dune resort condominiums to the start of the Zmudowski State Beach (Figure 3).

Pajaro beach is also unique in that there are few human influences (e.g., roads, infrastructures) or rocky headlands in the vicinity of the breach that play factor in shaping its morphology: A rocky barrier (riprap) to the northeast where a condominium exists, and a farm dirt road on the landward side of the lagoon are the primary geological features nearby. To the south of the lagoon area, there are larger (approximately 20 m) natural dunes, a common feature to Monterey Bay. The dune heights at Pajaro beach have

increased over the years by natural and man-made means to prevent flooding to the local community (river breaching has never occurred at the condominium proper). The river is managed and monitored by the County of Santa Cruz, Flood Control and Water Conservation District – Zone 7 (Barker 2022). The beach itself typically requires minimal management except for flooding risks, which is a major concern for the communities upstream of the Pajaro lagoon during significant storms, as witnessed in January and March of 2023 (Figure 4).

This research compares the water years (WY) 2022 and 2023 (normal and heavy precipitation years, respectively) to quantify the migration rates under variable river discharge and wave forcing. By measuring the Pajaro river discharge rates, wave radiation stresses (S_{xx} and S_{xy}), inlet mouth migration, significant wave heights (H_s), and sediment transport, a predictable trend can be deciphered that may be applicable to ephemeral rivers and other irregular inlets around the world. It is hypothesized that high discharge is required for longer inlet migration distances and prolonged seasonal opening of the Pajaro River breach. This paper introduces three hypotheses regarding the Pajaro river mouth breach migration: a) high river discharge affects inlet migration and promotes longer breached times, b) the annual breach time period for a normal (dry) season is from November to September but longer for a wet season, and c) the primary forcing mechanism at each period within that breaching season.

Figure 3. Pajaro River resorts and Zmudowski State Beach. Adapted from Google Earth (2023).

Figure 4. Aerial photos of the City of Pajaro flooding. Source: Jimenez (2023).

III. METHODS

A. METHODS OVERVIEW

Data for this research was collected via several methods over a span of October 2021-September 2023 to assess rates of morphological evolution. Collection of high resolution, georectified images were captured using three different UAS drones all with different payloads: the Alta X, DJI Inspire, and the DJI Mini 3 (the latter two of which are covered in Section F). The following sections describe each component along with their synthesis for analysis.

B. PAJARO FIELD RESEARCH SITE

The Pajaro River was selected for the study as it is one of California's several ephemeral rivers, and, unlike others, it is one of the few ephemeral rivers where the breach migrates in only one direction before closure. The Pajaro River watershed is approximately 1,300 square miles and supplies water to Santa Cruz, San Benito, Santa Clara, and Monterey Counties (Bijoor 2019). The Pajaro River feeds into Monterey Bay as shown in Figure 5. The river remains open most of the year. Closures typically occur when the river mouth migrates to the very southern end of the breach or during drier periods of the year.

Pajaro River discharge (d_r) and river height (h_r) was collected from the United States Geological Survey (USGS). The river gauge, located in Watsonville, CA, is approximately 4.5 miles upstream from the Pajaro River beach. Significant wave height (H_s), was acquired from Coastal Data Information Program (CDIP) site MO921. CDIP is a model hindcast that uses Simulating Waves Nearshore (SWAN) to predict wave shoaling and refraction along the entire California coast. Derived wave variables, specifically onshore wave radiation stress (S_{xx}), and alongshore wave radiation stress (S_{xy}), were computed resulting from these model outputs. It should be noted that mid 2023, CDIP deployed an observational buoy near MO921 site, and data compare well to model hindcasts. However, since the data does not span the entire observation period for this study, model outputs were used for consistency

Figure 5. Monterey Bay (center) and Pajaro River Beach (top right). Adapted from Google Earth (2023).

C. TOPOGRAPHIC (WALKING SURVEY)

Topographic surveys were conducted using a Spectra Precision SP60 Global Navigation Satellite System (GNSS) receiver using a modified backpack outfitted to firmly secure the receiver as in Figure 6. Data collection from the GNSS is 1 Hz with an accuracy of approximately 3 mm for both horizontal and vertical deviation. Elevation variations between users were measured and accounted for during post processing, which will be covered in Section H. For continuity, all walking surveys were conducted as uniformly as possible by walking along the water's edge first followed by either a zigzag or lawnmower pattern on the interior beach. Accurate walking surveys were conducted from January 2022–September 2023. For this research, the estimated error of the walking surveys conducted bi-weekly was assessed to be ± 10 cm. This error was introduced from the general walking motion, from how securely fixed the GNSS modified backpack was to the individual, sloping dunes of the beach, and the varying sand depths.

Figure 6. Survey backpack with GNSS

D. GPS GROUND CONTROL POINTS

Ground control points (GCPs) are giant white pieces of cardboard that are easily visible when viewing them from the lens of our UAS drones. They are necessary for georectifying the images and videography captured by the drones. The GCPs were strategically placed over the beach and river mouth survey area with an emphasis on being in the UAS Field of View (FoV). GCPs were placed on the beach prior to UAS flights. The Spectra Precision SP60 GNSS receiver was used to map each GCP location in order to ensure an accurate Global Positioning System (GPS) position was secured. To achieve an accurate GPS location, the GNSS was centered atop each specific GCP point for 5–6 mins. GCP placement was evenly distributed approximately 15 meters apart in either a triangle or zigzag pattern along the river mouth breach and inland on the beach/dunes. Avoiding linear placement and having all GCP points in the UAS FoV was paramount for imagery post processing as will be discussed in Section G.

E. ALTA X WITH LIDAR PAYLOAD

The Alta X is a quad-rotor UAS drone that can carry up to 33 lbs of payload. For this research, the payload included a 10 lbs. RIEGL Light Detection and Ranging (LiDAR) system and a Sony Alpha 7 RIII mounted below the LiDAR (Figure 7). The Alta X is powered by two top-mounted lithium-ion batteries. Average flights time with our payload was 15–17 mins before a battery swap was required. All flights were preprogrammed using the software application Alta Q Ground Control. In Alta Q Ground Control, an operator sets the waypoints, speed, and altitude over the desired flight path. Before the preprogrammed flight could commence, dynamic calibration was required to ensure proper function of the LiDAR system. This involved hovering the drone at an altitude of 50 meters then flying full throttle forward and reverse in a cross-type pattern. The dynamic calibration was performed twice: once before mission start and again after mission conclusion. Takeoff, landing, and dynamic calibration were flown manually with the use of a Futaba remote controller (Figure 9). Q Ground Control was the primary device for initiating mission start, which engaged full autonomous control. Manual control could be taken at any time in flight as long as the Futaba remote control was in range of the Alta X. During autonomous flight, all aspects of the mission and drone status were observed via Alta Q Ground Control on the mission building laptop.

Data processing was accomplished using three separate software programs: Applanix POSPAC, RIEGL RiProcess, and Quick Terrain Modeler (QT Modeler). All data from the flights is saved on a storage chip in the LiDAR system, which can be removed post-flight and downloaded to a computer for post processing. POSPAC was used to import the raw point cloud. A base station was also added in POSPAC so the LiDAR point cloud can have a stationary georeferenced location. Base stations can either be added manually, or a fixed GPS location in the vicinity can be used. For the manual location we used our Spectra Precision GNSS, and for the fixed, remote GPS location we used station National Oceanic and Atmospheric Administration (NOAA) Continuously Operating Reference Station (CORS) P210. NOAA CORS stations provide GNSS data that supports three-dimensional positioning, meteorology, and geophysical applications throughout the United States (NOAA CORS Website). Station P210 is a permanently grounded GNSS fixture

used for accurate GPS referencing. P210 is located in Watsonville, CA and is approximately 8 km from the Pajaro River beach site. Having both our own base station via the Spectra GNSS and a local CORS station provided redundancy should one option be unavailable. After importing the point cloud and establishing the base station, we were able to move on to the RiProcess application.

RiProcess was used to quality control the raw data into a usable product, by removing data with false return information (i.e., off sea spray and foam). This is where most of the analysis can be completed. All raw LiDAR point cloud data sets collected required some editing to remove any erroneous outliers from the returns. RiProcess allowed us to crop out the bad data, combine the data points of the point cloud into a smooth, cohesive picture, and export the finished product. Unfortunately, RiProcess does not offer kml/kmz as an export option. In lieu of this, QT Modeler is used to export the data into a kml/kmz file required for import into SMS. Due to licensing issues, we could not import our raw point cloud data into QT Modeler from start to finish of data processing. An example of the final product can be viewed in Figure 8.

Figure 7. Alta X with LiDAR and camera payload

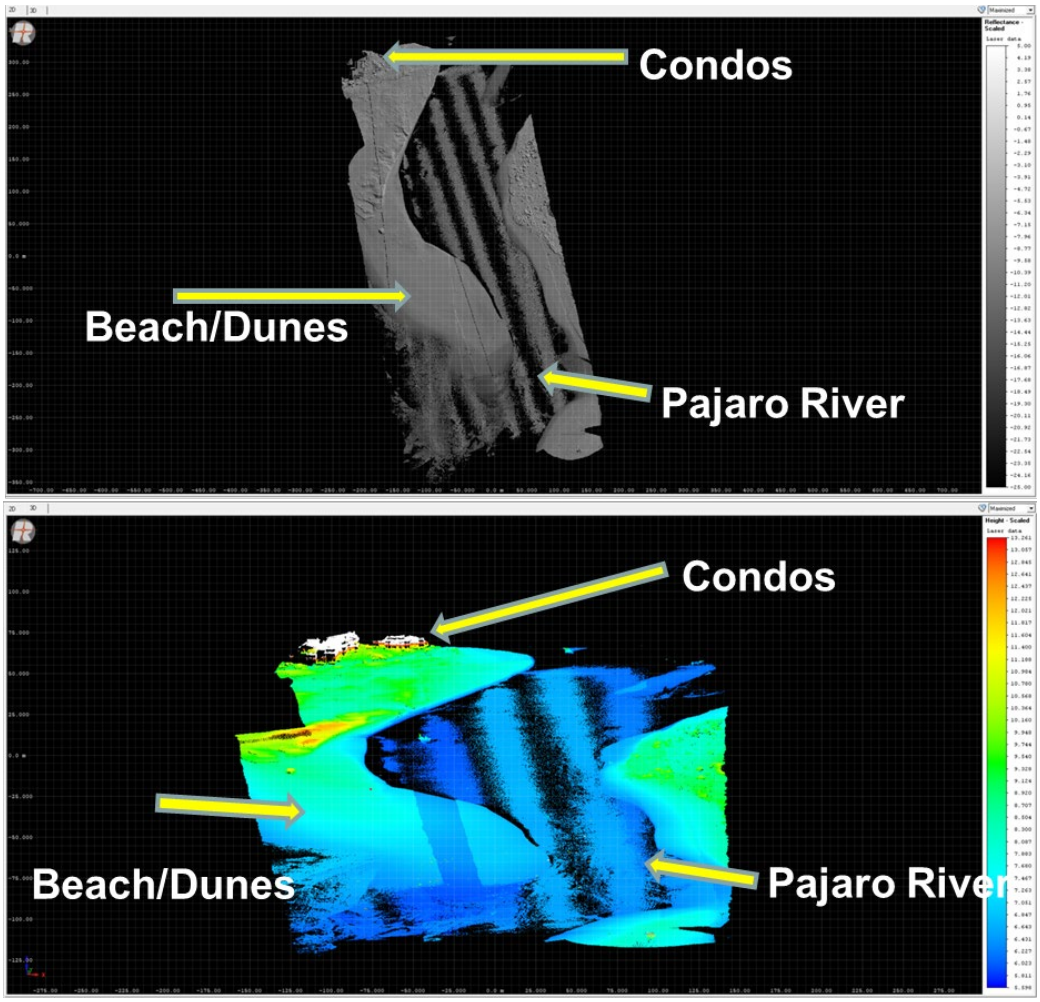

Figure 8. LiDAR scans of Pajaro River Beach

Figure 9. Futaba handheld Alta X remote controller

F. IMAGERY UAS SYSTEMS: DJI INSPIRE AND DJI MINI 3

Overhead imagery and videos were captured using two DJI UAVs as seen in Figure 10, the Inspire 1 and the Mini 3. The Inspire 1 is approximately 6.5 lbs, uses lithium polymer batteries, and has a gimbal style camera system. Max flight times was around 15 minutes before a battery swap was required. The purpose for the Inspire was to capture 5–7 minutes long hovering videos that captured all of the GCP's on the beach in order to create georectified images and videos.

At just over 0.5 lbs., the Mini 3 uses lithium-ion batteries, and has a gimbal style camera system used for scouting the beach area prior to setting up/deploying the larger UAVs. Additionally, the Mini 3 was ideal for taking photographs of the Pajaro River beach and breach location due to its small size and quick deployment capability.

Figure 10. DJI Inspire 1 (left) and DJI Mini 3 (right)

G. COASTAL IMAGING RESEARCH NETWORK (CIRN)

Coastal Imaging Research Network (CIRN) is a software application used to automatically orthorectify the Inspire UAV's video imagery. Using CIRN's Quantitative Coastal Imaging toolbox along with MATLAB, the images were translated from a three-dimensional area to a two-dimensional cartesian field (Plant 2022). Since the process is not always perfect in its placement minor adjustments are made by using the GCPs to align the images to their correct orientation. After the corrections were made, the images were then exported as a PNG file to be used for follow-on analysis that will be covered in Section I.

H. SATELLITE IMAGERY COLLECTION

Satellite imagery of the Pajaro River over a two-year time span was obtained from two sources: Sentinel-2 and Google Earth. Due to the low frequency of updates for Google Earth imagery, Sentinel-2 was the primary source of satellite imagery collection.

The Sentinel-2 L2A satellite covers 13 different bands of the electromagnetic spectrum. The images collected for this research fell in the True Color bands 2 (red), 3 (green), and 4 (blue) with a spatial resolution of 10 meters. The True Color bands gave a natural-colored product that best represents the Earth's surface and was determined to be the best for river mouth breach migration analysis. The images were downloaded as high-resolution PNG files to be used in follow-on analysis software.

I. AQUAVEO SURFACE-WATER MEASURING SOFTWARE (SMS)

Aquaveo Surface-Water Measuring Software (SMS) is a modeling and visualization software application that aids in conducting measurements and analysis on coastal environments. SMS allowed us to conduct time-lapsed measurements for our two-year span of data collection. We focused mainly on the southerly migration of the Pajaro River breach into Monterey Bay, but SMS allowed for measuring sediment height migration and cross-shore length variations as well.

SMS supported all forms of data collection that were used in this research and allowed for compiling of all data points into one database for analysis. The Sentinel-2 satellite images were imported as KMZ files, the LiDAR as dem files, and the CIRN images

as PNG files. The walking survey data was imported into SMS and post processed directly through the software into georectified sediment transportation information that was used for beach inlet migration measurements. Since walking surveys provide single-point location data along the path being walked, gaps exist which SMS can interpolate at selected horizontal resolution giving accurate sediment heights anywhere in the area of collected data. Since this research is mainly concentrated on the border of the walking surveys where topographic data exists, interpolation error is not required.

In order to accurately measure and compare all of our data sets in SMS, a mesh grid with 10 m spacing was created parallel to the beach starting from the riprap in front of the Pajaro Dunes condominiums and expanding to the Zmudowski State Beach as seen in Figure 11. This spacing was chosen because it matched the 10 m resolution of Sentinel 2 satellite images, which was the lowest resolution of all of the data sets collected. We overlayed each data set on top of the grid. Weather and equipment permitting, data was captured at least twice a month or every two weeks. Using the SMS measuring tool, we calculated the cross-shore and longshore distances for that given day and recorded the results. Certain days only had one data source (ex: only Sentinel 2 image), while others had multiple (ex: LiDAR, walking survey, CIRN, and Sentinel 2). The days with multiple data sources allowed for the most comparison when taking measurements of the Pajaro River breach migration.

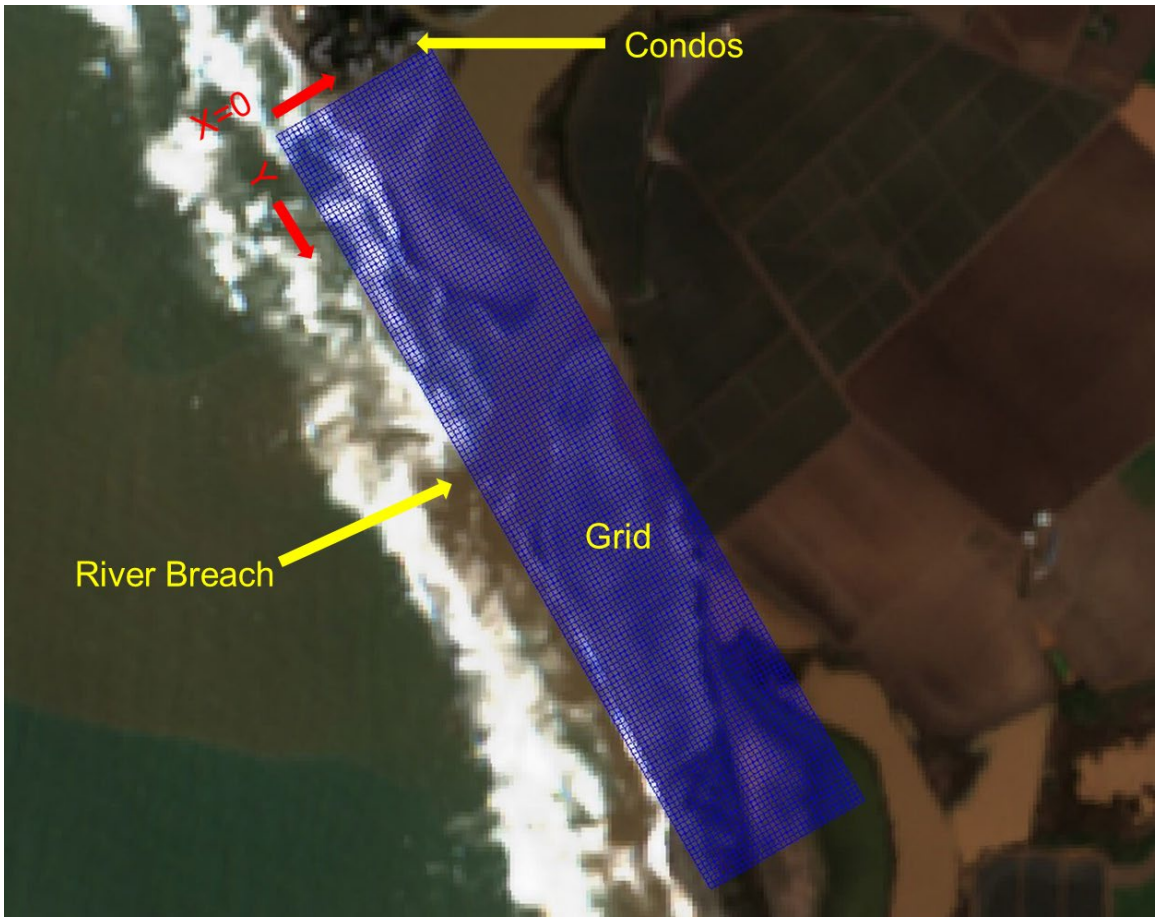

Figure 11. Sentinel-2 satellite imagery in SMS. Adapted from Sentinel-2 (2023).

IV. ANALYSIS

A. KEY ASSUMPTIONS

Measurements taken on SMS were done using the measurement tool and lined up inside the 10 m resolution grid where the origin was located at the riprap protective barrier at the northern end of the beach (Figure 11). Due to the low 10 m resolution of the Sentinel satellite images, some of the measurements of the actual breach location are estimated to have an error of ± 20 m for days where Sentinel satellite images were the only available data source. This error is well within a comfortable confidence interval and the overall trend of the data remains unchanged giving sureness in the reliability of this study's conclusions. Walking surveys were taken at varying tidal ranges which was observed to influence breach migration rates on days when surveys were taken at the low or high extremes of the tidal cycle. This did not appear to affect the overall migration rate or direction, but the migration rates are observed to drastically vary daily depending on the tidal cycle. This is very evident in WY 2023 migration rates from April to September as the reader will see later in this chapter. To ensure consistency, all SMS measurements were taken at the furthest point of the north side of the Pajaro River beach opening as referenced to the longshore grid. Breach migration often did not occur along the same bearing and was evident in our field work. This means that the breach would often move onshore or offshore in addition to longshore. For the purposes of this study, the WY is defined as 01 October to 30 September, which is consistent with seasonal breaching and closing patterns of both years.

B. 2022 WATER YEAR

Figure 12 shows the river migration progression for this year, over which all breaches and closures were natural with no outside influence. The total southerly migration for WY 2022 was 222 m. Measurements of the breach location are shown in Figure 13a. This element is key to this study as we will be comparing WY 2022 and WY 2023 in Chapter V where neither year had any mechanical breaches. Additionally, this study defines 2022 as a normal water year, meaning that there were no unusual atmospheric

events that caused major changes in the surrounding community or the Pajaro River itself. The Pajaro River typically follows a cyclical trend year to year where breaching occurs in the winter from increased precipitation and river discharge and generally closes toward the end of the following calendar year (late summer-fall) when less rain and river discharge are present. Water year 2022 had three natural breaches and three closures. The initial breach occurred on 25OCT2021 and closed on 29OCT2021. The following breach occurred on 13DEC2021 and remained open until 06MAY2022 where there was a four-day closure. Upon opening on 10MAY2022, the river remained open until its final closure of the water year on 19SEP2022. The mechanisms for all of three natural breaches were wave overtopping either due to storm surges (25OC2021 and 13DEC2021) or transition in the tidal season (10MAY2022) (Barker 2022).

Figure 12. Water year 2022 progression. Drone photography provided by Dr. Mara Orescanin and Rusty Barker.

1. Pajaro River Discharge for Water Year 2022

The Pajaro River discharge rates for the 2022 water year can be seen in Figure 13b. During the initial breach of the 2022 water year on 25OCT2021 (vertical dashed lines, Figure 13) spikes can be observed in the river height (h_r) to 4.8 m from the average 3.2-3.3 m over the previous few weeks. Additionally, the river discharge rate (d_r) shows a drastic

increase from the average of 0.01 m^3/s to 11.9 m^3/s during this time. After this breach, both h_r and d_r return to their preceding averages, four days prior to an observed beach closure on 29OCT2021 (vertical solid lines, Figure 13). A small rise in both d_r (1.5 m^3/s) and h_r (3.8 m) are observed again on 09NOV2021, but no resultant breaching occurred, and the values returned to normal. On 13DEC2021 the lagoon naturally breached again, and an elevated d_r of 21.2 m^3/s and h_r of 5.2 m was observed a couple of hours after the breach. During December of 2021, the discharge rate and river height are observed fluctuating drastically day to day with the annual maximum discharge rate of 40.5 m^3/s and height of 5.8 m occurring on 28DEC2021. Both numbers are the highest values observed for the entire WY 2022. After this, the river remained open except for a 4-day closure that occurred on 06MAY2022 that was not accompanied by the previously seen spikes in h_r and d_r making closure difficult to predict. The values at the time of closure were 0.2 m^3/s for d_r and 3.5 m for h_r. The river breached four days later on 10MAY2022 with a slight decrease in river discharge rate (0.1 m^3/s) and height (3.3 m). The river remained open for the next 3.5 months with discharge rate and river height values holding constant around 0.2 m^3/s and 3.2 m respectively. The final closure ending WY 2022 occurred on 19SEP2022 with a small spike in river discharge (1.6 m^3/s) and river height (3.9 m).

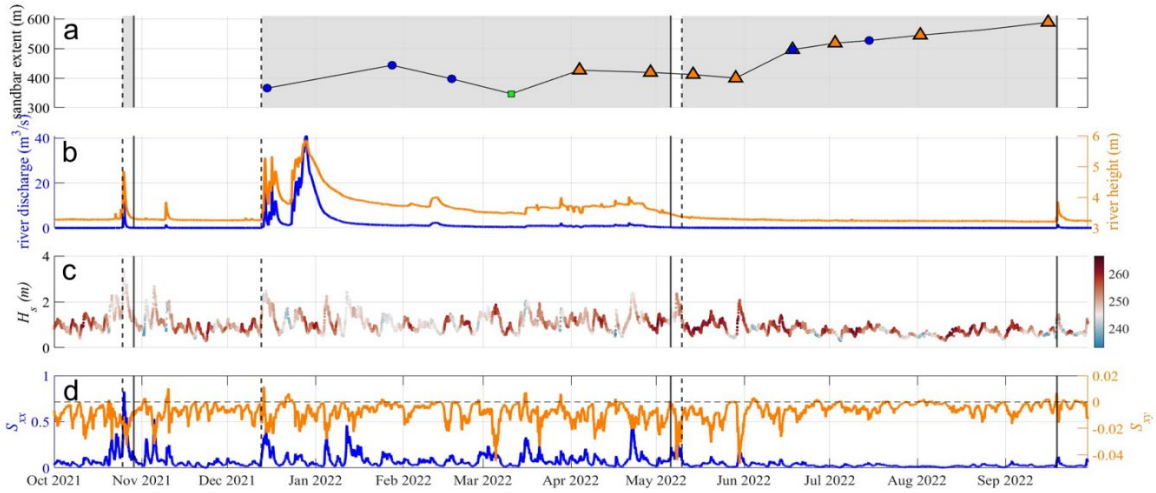

Part (a) is the sandbar migration extent in m. The y-axis is oriented from north on the bottom to the south on the top. This details the overall breach migration from north to south over the water year (x-axis). The symbols and color indicate the method of data collection: blue circles (walking survey), green box (CiRN), orange triangle (Sentinel satellite), blue triangle (walking survey and Sentinel satellite). Part (b) is the Pajaro River discharge rate (blue) along with the river height (orange). Part (c) is the significant wave height, H_s, with the wave direction indicated by the color bar on the right y-axis. Part (d) is the onshore component of wave radiation stress, S_{xx} (blue), and the alongshore component of wave radiation stress, S_{xy} (orange). Part (b) data was acquired from the United States Geological Survery (USGS). Part (c) and (d) were acquired from the Coastal Data Information Program (CDIP) site MO921.

Figure 13. Water year 2022 (1. Sandbar migration vs. time; 2. River discharge vs. river height, 3. S_{xx} vs. S_{xy}; 4. H_s vs. wave direction)

2. Significant Wave Height, Wave Direction, and Wave Radiation Stress Water Year 2022

Figure 13c displays the offshore wave direction and H_s for water year 2022, and Figure 13d displays the cross-shore (S_{xx}) and along-shore (S_{xy}) wave radiation stress, where wave information comes from the Coastal Data Information Program (CDIP) hindcast model outputs for location MO921 in 15 m water depth. The radiation stress representing the flux in the *x*-direction of the x component of momentum (the cross shore wave radiation stress) is defined as

$$S_{xx} = E[n(sin^2\theta + 1) - \frac{1}{2}]$$

The flux of x momentum in the y direction (the along shore wave radiation stress) is defined as:

$$S_{xy} = \frac{EnSin2\theta}{2}$$

The angle, Θ, for both wave radiation stress equations above is defined as the angle the wave direction makes with the x-axis and this assumes that waves are traveling in the x direction (Dean and Dalrymple 2002). This is a measure of wave obliqueness, i.e., how refracted the waves are at the coast, and Θ=0 for fully refracted waves.

The energy density term, *E*, in both equations is:

$$E = \frac{1}{8}\rho g H^2$$

where ρ is the water density, g is the acceleration due to gravity, and *H* is wave height. Additionally, n is a function of depth and is defined as:

$$n = \frac{1}{2}\left(1 + \frac{2kh}{sinh2kh}\right)$$

The term n is 0.5 for deep water and is 1 in shallow water. The wave number, k, is equal to $\frac{2\pi}{L}$ where L is the wavelength.

Of note, all of the equations listed above are standard definitions sourced from Coastal Processes with Engineering Applications (Dean and Dalrymple 2002).

Figure 13c represents significant wave height (H_s) and direction (σ) during the 2022 water year oriented shore normal (245° compass bearing) to the Pajaro River beach. Observing the H_s plot, maximum value is just over 3.3 m with a wave direction of 239° taken on 25OCT2021 corresponding to the initial breach of the 2022 water year. Of note, the wave direction overall maintains a fairly shore normal orientation with few deviations north and south of 245° until substantial weekly changes in direction are observed around early May 2022. After the 06–10MAY2022 closure, *H*s has another small peak of slightly

over 2 m on 30MAY2022 followed by stabilization of around 1 m. One final peak of H_s = 1.44 m is observed on 19SEP2022 corresponding to the final closure of WY 2022.

Figure 13d shows that the onshore radiation stress (S_{xx}) is always positive and associated peaks accompany increased river discharge, river height, and *H*s increases as per Figure 13b and d. This indicates increased forcing in the x direction during times of peak discharge and wave heights. For the along shore radiation stress (S_{xy}), almost all values are negative throughout the 2022 water year indicating a predominate southward forcing along the Pajaro River beach.

C. 2023 WATER YEAR

The single breach during this year occurred naturally with no outside influences, and likewise, no closures, natural or artificially induced, occurred during the 2023 water year. The initial breach occurred on 25NOV2023 and the Pajaro River remained breached throughout and into the beginning of WY 2024 as of the writing of this paper. The furthest southerly migration distance was 771.5 m. The river migration progression for WY 2023 can be seen in Figure 14.

Figure 14. WY 2023 progression. Drone photography provided by Dr. Mara Orescanin and Rusty Barker.

1. Pajaro River Discharge for WY 2023

The Pajaro River discharge and height in Figure 15b shows d_r and h_r remained fairly constant from the beginning of the 2023 water year until early December 2022 with values averaging $0.01 m\text{^}3/s$ or less for discharge and 3.2-3.3 meters for height. There were two exceptions for this occurring on 01NOV2022 ($d_r = 1.91\ m\text{^}3/s$ and $h_r = 3.9$ m peak values)

and 08NOV2022 (2.66 $m\text{^}3/s$ and 4.1 m peak values). However, the breach remained closed during these small spikes in values. During and shortly after the initial breach on 25NOV2022, both the river discharge and river height remained constant at their initial averages at the start of the water year as listed above. From 01DEC2022 through most of January 2023, there are multiple spikes in discharge and height with the peaks for both values during the two months occurring on 10JAN2023 (291.69 $m\text{^}3/s$ and 9.57 m respectively). Between 28JAN2023 to 24FEB2023, the values, although well above their typical averages, are observed to stabilize (4.3-5.1 m for h_r and 5.6-19.1 $m\text{^}3/s$ for d_r). After 24FEB2023, multiple high peaks in both values are observed on 02, 11, 23, and 30 March with the greatest values for the year happening on 11MAR2023 (9.78 m for h_r and 331.34 $m\text{^}3/s$ for d_r). In addition to being the highest values for March 2023, these values were also the highest observed for the entire WY 2023. From April until the end of WY 2023, both discharge and height stabilize with no more sharp increases for either. Although higher than the beginning of the year average, the river height remained constant with values between 3.5-3.6 m. The river discharge, however, a drastic drop was observed from MAY2023-SEP2023 from where it returned to the beginning of the WY averages from OCT2022-NOV2022 with values ranging from 0.1-0.3 $m\text{^}3/s$.

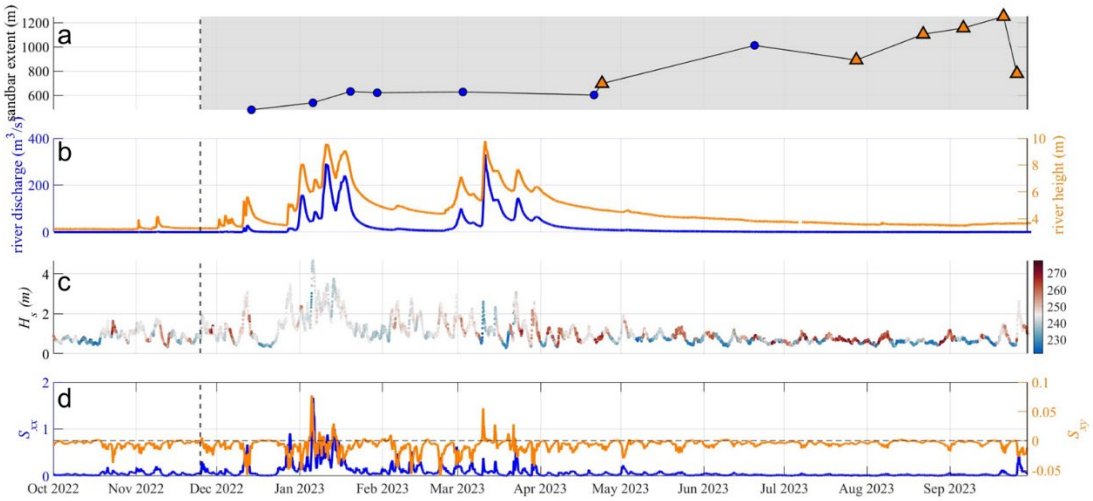

Part (a) is the sandbar migration extent in m. The y-axis is oriented from north on the bottom to the south on the top. This details the overall breach migration from north to south over the water year (x-axis). The symbols and color indicate the method of data collection: blue circles (walking survey), orange triangle (Sentinel satellite). Part (b) is the Pajaro River discharge rate (blue) along with the river height (orange). Part (c) is the significant wave height, H_s, with the wave direction indicated by the color bar on the right y-axis. Part (d) is the onshore component of wave radiation stress, S_{xx} (blue), and the alongshore component of wave radiation stress, S_{xy} (orange). Part (b) data was acquired from the USGS. Part (c) and (d) were acquired from CDIP site MO921.

Figure 15. WY 2023 (1. Sandbar migration vs. time; 2. River discharge vs. river height, 3. S_{xx} vs. S_{xy}; 4. H_s vs. wave direction)

2. Significant Wave Height, Wave Direction, and Wave Radiation Stress for WY 2023

Figure 15c represents H_s and Θ (peak wave direction) during WY 2023. Similar to WY 2022, WY 2023's also shows wave direction oriented shore normal to the Pajaro River beach during winter months (OCT2022-APR2023) with increasing oblique angles in summer months (MAY2023-SEP2023). Observing the H_s plot on 25NOV2022, the H_s has a small spike with a value just over 1.9 m with a wave direction of 241°. This date corresponds to the initial breach of the 2023 water year. From December 2022 to the end of March 2023, H_s had several significant peak values. The highest Hs value was 4.66 m on 06JAN2023. This was also the highest value recorded during the WY 2023. The wave direction maintains a fairly shore normal orientation with few deviations north and south of 245° until substantial weekly changes in direction are observed around the middle of

March 2023 and are maintained throughout the remainder of the water year. From 01APR2023 to the end of WY 2023, H_s values stabilize and range from 1 to 1.9 m heights. The one exception occurred on 26SEP2023 where H_s spiked to 2.62 m, which may play a role in why there is substantial northward migration in the last weeks of SEP2023.

In Figure 15d, it is observed that S_{xx} is always positive and associated peaks are in line with the increased H_s increases as well (Figure 15b & c respectively). This indicates increased forcing in the x direction during times of peak wave heights. For S_{xy}, almost all of the values are negative throughout WY 2023 with exceptions being for a few instances between 05–13JAN2023, 03–04FEB2023, and 10–21MAR2023. January and March have high river discharge, river height, and increased H_s. However, it is the high wave height combined with peak wave direction from the southwest that leads to the positive values for S_{xy}, a factor only observed in the winter season. February does have increased H_s, but not coincident with wave direction from the south compared to January and March. This could explain why the S_{xy} value is mostly negative and smaller in magnitude compared to the positive peaks seen in January and March. Overall, the average longshore wave stress is from north to south along the Pajaro River beach during the majority of the water with the exceptions being the few dates listed above.

THIS PAGE INTENTIONALLY LEFT BLANK

V. COMPARISON OF WATER YEARS 2022 AND 2023

A. BREACH AND CLOSURE DISCUSSION

WY 2022 and WY 2023 offer a great comparison for river beach migration because both years had natural beach breaches but have very different environmental forcing. Initial breaches for both years was 25OCT2021 and 25NOV2022 respectively, though for WY 2022, the initial breach closed after four days and the seasonal transition to open occurred at the second breach in December. For this study, inlet location measurements began within three weeks of seasonal transitions to fully open. They occurred almost one year apart: (15DEC2021 and 14DEC2022) for each water year. One interesting observation is that the breach on 25OCT2021 and 13DEC2021 were close to the same location (Barker 2022). The initial breach measurement for WY 2022 was 365.9 m and 478.4 m for WY 2023. Even though there is a 113 m difference, both natural breaches occurred roughly at the same time and location as can be seen in Figure 16. The fact that the breach in WY 2023 occurred farther north than the closure from WY 2022 suggests breaching and closure affect the inter-annual migration rates. This is likely owing to uneven beach berm elevation development during the closed season and deserves further study.

Figure 16. Initial breach locations for WY 2022 and WY 2023

As previously discussed in the Analysis chapter (Chapter IV.B), WY 2022 had three openings and closures, whereas 2023 remained open after its initial breach, and is still open at the date of this work. The number of closure days for WY 2022 was 85 days spread with the majority of the days falling at the beginning of the WY. The closure days for WY 2023 was 30 days less at 55. All of these days were accounted for before the initial breach on 25NOV2022. A comparison of both WY's and the differences in magnitude can be observed in Figure 17.

	WY2022	WY2023	Difference
Total Rain	0.68m (26.8")	1.35m (53.1")	2x
Max River Discharge	40.5 m^3/s	331.3m^3/s	10x
Max River Height	5.8m	9.8m	2x
Average Migration Rate	0.7 m/day	5.5 m/day	5x
Winter Migration Rate	(-)0.16 m/day	1.56 m/day	(-) vs (+)
Summer Migration Rate	1.73 m/day	8.68 m/day	4x
# of Days Closed	85	55	-30

Figure 17. WY 2022 and WY 2023 comparison

B. RATES OF MIGRATION

1. 2022 Water Year

The average daily rates of migration as well as the net migration between the WY 2022 and WY 2023 vary quite drastically. Daily migration rates are calculated as a function of time by comparing breach position over the observation interval. As can be seen from Figure 18, WY 2022 fluctuates between northward and southward migration during the winter months (DEC2021 -MAY2022) when river discharge is high but variable, and wave angle is close to shore normal. Rates of migration range from -2.4 to 3.3 m/day with positive values indicating southward breach migration and negative being northward. The overall average migration southward during the open inlet state is 0.7 m/day as indicated by the red line on Figure 18. The green and magenta lines represent the rates of migration during the winter and summer months respectively. During the winter months (green line), the rate of migration is slightly negative at -0.16 m/day and the migration of the Pajaro breach is both northward and southward, with an overall net trend slightly northward. During the summer months, the migration pattern stabilizes with a steady southward trend and the rate of migration increase to 1.73 m/day as annotated by the magenta line in Figure 18(a).

After the brief four-day closure in May 2022, the rate of migration steadies after a large 4.8 m/day rate of migration jump from May to June 2022. As stated in the Methods section, data was collected at varying tidal times throughout the day. The low tide for the

day was 0854 PST, and it is estimated that the Sentinel-2 image where the data was measured from was taken approximately one hour after low tide the morning of 18JUN2022. This might suggest an overestimate of the rate of migration from 29MAY2022 to 18JUN2022. The remaining three and a half months of WY 2022 show an almost constant rate of migration ranging between 0.9 to 1.4 m/day, as well as a steady migration southward until ultimate closure on 19SEP2022. The ultimate trend of migration for WY 2022 is southward with the initial measurement taken being 365.9 m and the final before closure 587.9 m for a total southward breach migration of 222 m. Of note, 587.9 m was also the farthest southward migration distance measured for the WY.

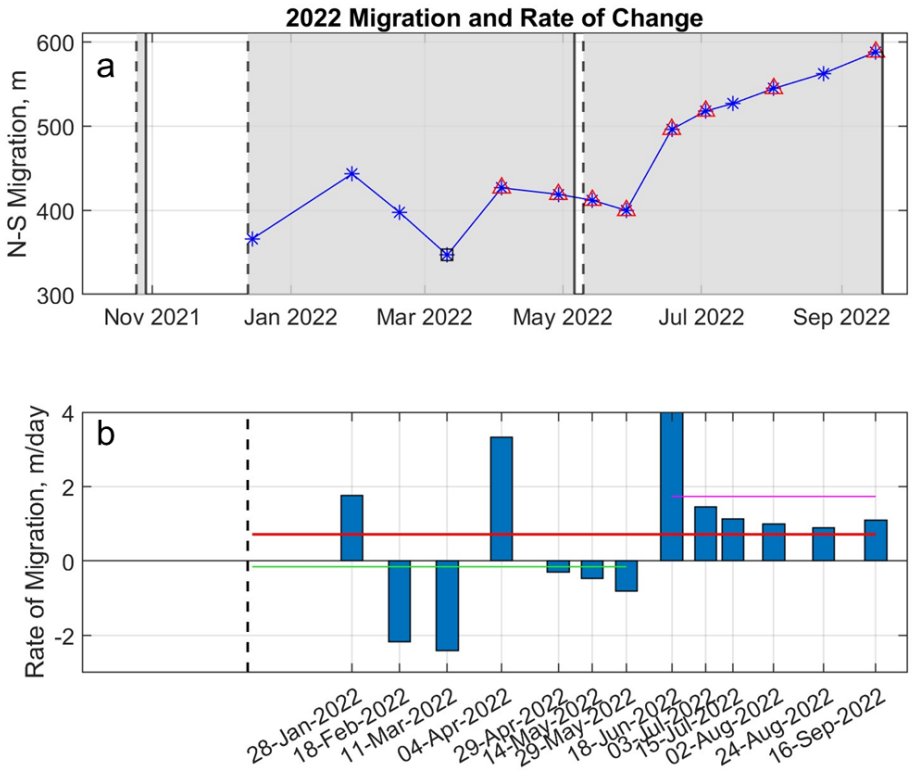

Part (a) is the sandbar inlet migration distance in m. The symbols on the line indicated the method of data collection for that particular day. The (*) indicate GNSS walking surveys, the box symbol represents CIRN data, the red triangle indicates satellite data, and a combination of both indicates multiple sources of the specified type were used. Part (b) is the calculated daily migration rate, where positive indicates migration to the south. The red line indicates the overall migration rate average for the entire WY. The green line indicates the average migration rate for the winter months while the magenta line indicates the average migration rate for the summer months.

Figure 18. WY 2022 migration (a) and rate of migration (b)

2. 2023 Water Year

WY 2023 displays a significant increase in migration distance as well as migration rate compared to the previous year (Figure 19). WY 2023 was a very unusual year in terms of the amount of precipitation that occurred and is therefore classified as a wet year compared to 2022 being a normal water year. The overall rate of migration for WY 2023 was 5.5 m/day, nearly 8 times that of WY 2022. As for WY 2022, an observable difference for the breach migration and rate of migration between the winter (OCT2022-APR2023) and summer (MAY-SEP2023) months is evident. The winter months (green line) has an average rate of migration of 1.56 m/day, and the breach migration southward is not as steady or stable as the second half of the water year. During the summer months, the rate of migration increases to 8.68 m/day and the breach migration stabilizes with a steady southward trend. Although the overall migration tends southward just as it did in 2022 with an initial breach measurement of 478.4 m and a final measurement of 777.8 on 26SEP2023, periods of northward and southward migration exist during the winter before switching to constant southward migration during the summer. The farthest southward migration measurement was 1249.9 m taken on 21SEP2023. The total southward migration prior to 26SEP2023 was 771.5 m, a 549.5 m increase from water year 2022.

Of note, there are two data points on Figure 19 that are considered to be anomalies. The dates are 24APR2023 and 26SEP2023. For 24APR2023, the measurement was taken via Sentinel-2 satellite imagery. Low tide occurred at 0854 PST, and it is estimated that the satellite image was captured within one hour of this time. This would explain the vast migration rate increase between 21APR2023 and 24APR2023, as the beach elevation are quite low, and suggests error estimates should account for tidal stage. For 26SEP2023, the northern edge of the breach caused channel rotation leading to elongation/formation of a beach spit, which developed where the breach migration measure were being taken from. Between 21SEP2023 and 26SEP2023, the spit had become very thin, and ultimately, cut off from the northern part of the beach by the Pajaro river and by the first large wave event of the fall. This was visible on Sentinel-2 satellite imagery and explains the sudden 472 m northward migration and the unusual -94 m/day rate of migration. In contrast, for WY 2022, these wave events occurred at roughly the same time of year, but the inlet was closed

and could not migrate. For Figure 19, 26SEP2023 was excluded from the rate of migration calculations on the figure for this reason. This suggests the consequences of wet years resulting in no summer closure may undo any net migration during the summer and may account for a "re-setting" of the system.

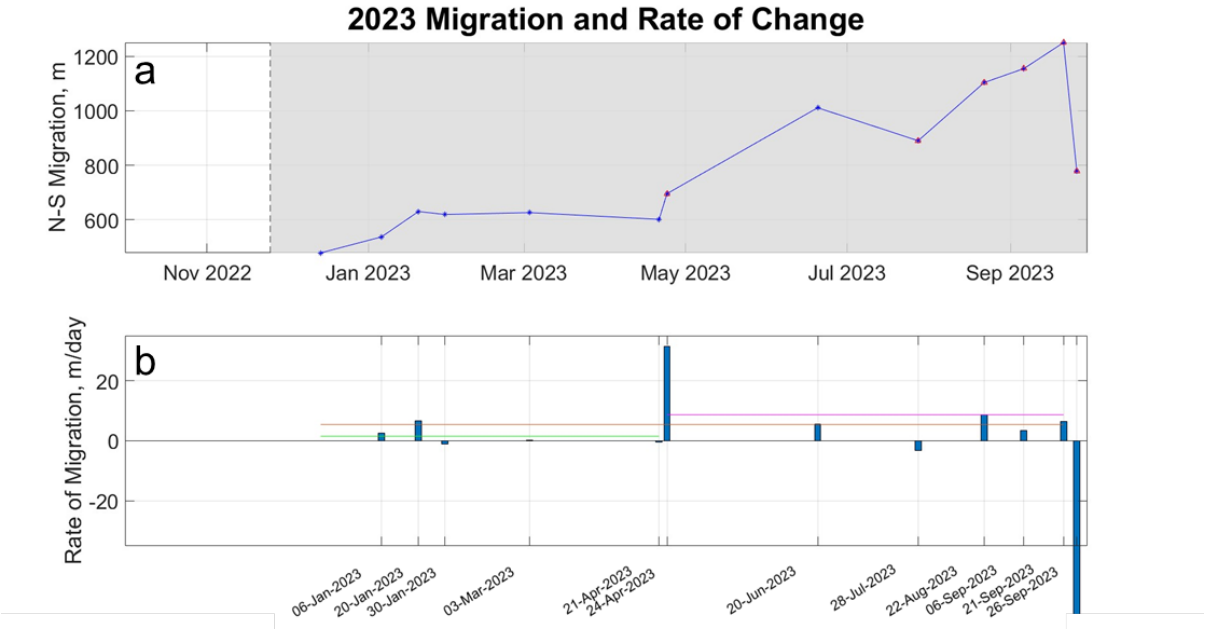

Part (a) is the sandbar inlet migration distance in m. The symbols on the line indicated the method of data collection for that particular day. The (*) indicate GNSS walking surveys, the red triangle indicates satellite data, and a combination of both indicates both sources of the specified type were used. Part (b) is the calculated daily migration rate, where positive indicates migration to the south. The orange line indicates the overall migration rate average for the entire WY. The green line indicates the average migration rate for the winter months while the magenta line indicates the average migration rate for the summer months.

Figure 19. WY2023 migration (a) and rate of migration (b)

C. WY2023, AN ANOMALY FOR PRECIPITATION

This study classifies WY 2022 and WY 2023 as dry versus wet with the wet year being the latter. Figure 20 shows the 2022 and 2023 water year total precipitation. The precipitation values were gathered from Santa Cruz One Rain station CORRALITOS RAWS (COR), which is located less than ten miles north of the Pajaro River Beach and is adjacent to Watsonville, CA (The County of Santa Cruz). The total amount of precipitation

for WY 2022 was 0.68 m compared to 1.35 m for WY 2023. For a magnitude perspective of how much rain WY 2023 received, WY 2021 had 0.61 m and WY 2020 had 0.41 m. The rainfall values for the past three years either doubled or were greater in WY 2023. Of note, the majority of the precipitation occurs in the winter months for both years up to March-April and then tapers off, which will be analyzed in the next section.

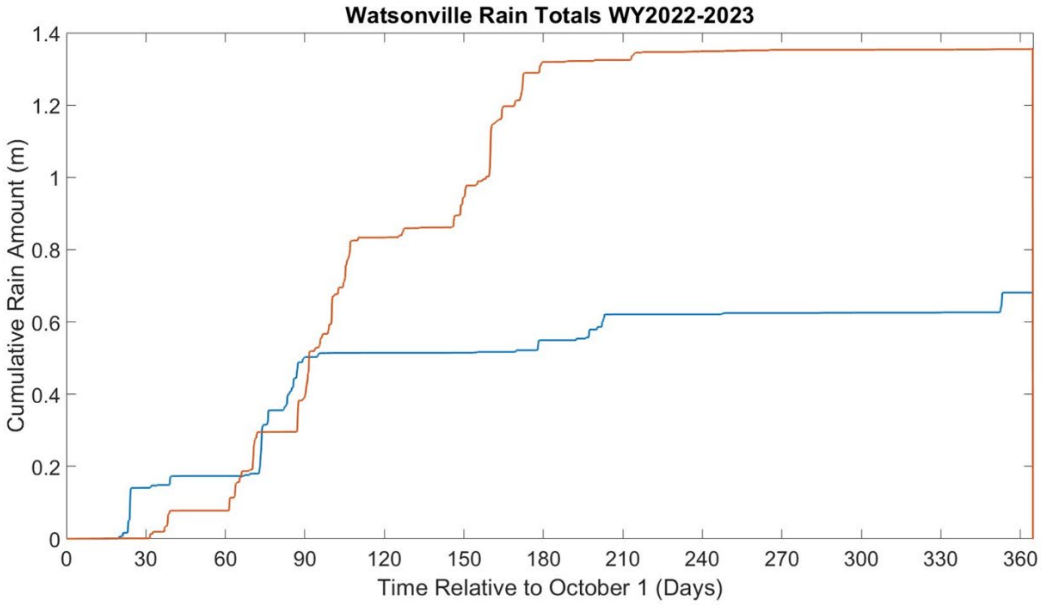

Figure 20. WY 2022 (blue) and WY 2023 (orange) rainfall totals (m). Data from Santa Cruz One Rain Station CORRALITOS RAWS (COR) ID: CA22D628.

D. CORRELATIONS BETWEEN VARIABLES DRIVING BREACH MIGRATION

This study examined many variables (S_{xx}, S_{xy}, H_s, river height, river discharge, and precipitation totals) that all contribute to the Pajaro River breach southerly migration. Ultimately, the aim is to be able to predict which factors play the biggest role in migration and compare the differences during a normal, dry year (WY 2022) and an unusual, wet year (WY 2023). Figure 21 shows the migration patterns for both years side by side. Both water years. Pajaro beach consistently breaches towards the north side of the beach naturally. When a mechanical breach is required, it is always performed to the north side

of the beach as well. Regardless, the breach migration consistently flows southward, with the majority of the migration occurring during the summer, until annual closure toward the end of the year water year. This pattern is evident in WY 2022 that showed three natural breaches and closures. WY 2023 shows a similar pattern but never closed and the migration is much farther than normal years. The patterns are very similar between the two waters, despite the magnitude differences. The flowing sections split up the analysis into the winter (wet) and summer (dry) to study the trends between them.

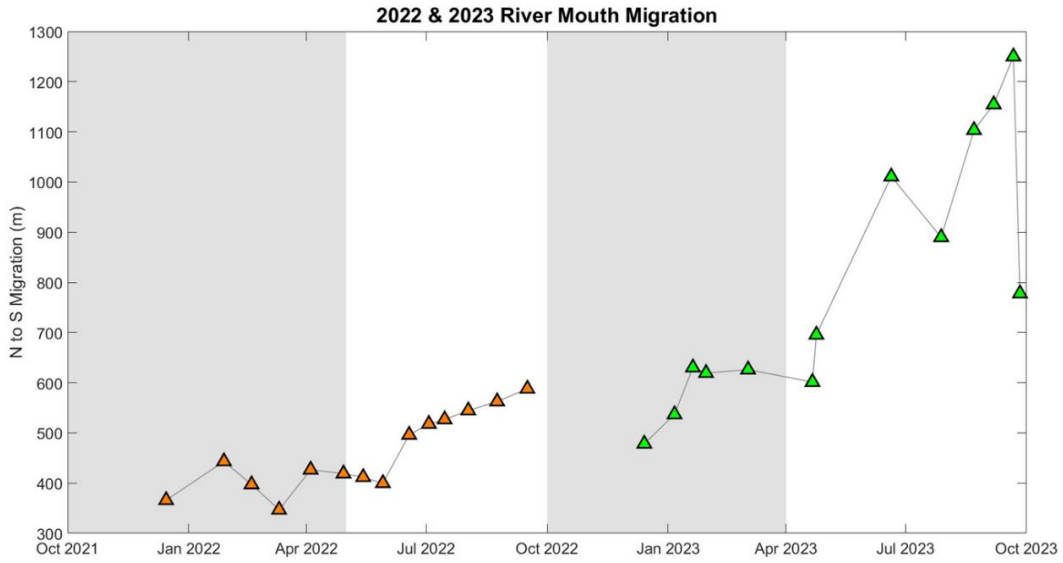

The shaded areas represent the respective winter months for both WY 2022 and WY 2023. The non-shaded areas represent the summer months for both WY's.

Figure 21. WY 2022 (left) and WY 2023 (right) overall southward migration trends.

1. Winter Months Migration (Wet Season)

Several patterns can be deciphered from analysis of all the factors listed above. Both water years have a similar trend for erratic migration in the winter months that stabilizes in the summer to steady southward migration. As can be seen in Figure 20, the majority of the total rain occurs for both years through the month of March. WY 2023 total rain is double that of WY 2022, which plays a factor in the values of river stage and

discharge, and relative strength compared to H_s and radiation stresses. Observing Figures 13b and 15b, take note that the scale for rate of migration for WY 2023 is a factor of ten greater than WY 2022, and that the river height is two times greater that WY 2022. Even with the vast differences in rain, river discharge, and river height, the large spikes for these values occur roughly at the same time in January. These can be attributed to the rain events for both years with the rain amounts contributing to the varying magnitudes. From December through January, the Pajaro river breach migration is directly affected by the strong river discharge rate and increased river height.

Figures 13c & d, and 15c & d display similar patterns with large spike in H_s with a near shore normal direction, large S_{xx}, and large S_{xy} values. The large increases in S_{xy} contribute to the small northward, or slowing of the southward, migration of the river breach that occurs in both years that begins at the end of January. From the migration patterns from February to the beginning of April for both years, it can be observed there is a northward breach migration trend for WY 2022 and much smaller northward trend for WY 2023. Both years have slightly positive values for S_{xy} and a shore normal wave direction, which explains the northward migration. However, WY2023 has a much higher river discharge rate and height, which is directly counteracting the northward wave radiation stress (S_{xy}) driven by an increased H_s and wave direction that is coming from 230° (15° less than shore normal) during peak S_{xy} values. WY 2022's values river discharge and height are not strong enough to counteract the positive S_{xy} and thus, results in a stronger northward breach migration during this two-month period.

2. Summer Months (Dry Season)

By the end of April to the beginning of May, around 90 percent of the total rain for the years had occurred signifying the switch to the dry season. Additionally, the peak wave direction changes significantly from being relatively shore normal during the winter months to varying ±25° from shore normal on a weekly basis. With this seasonal shift, the river breach migration pattern changes, but the trends for both years remains similar. From examination of all data points, it was determined that the shift to the dry season occurred during the last week of May for WY 2022 and the last week of April for WY 2023. This

was determined by examining the rain fall totals, shift in on shore wave direction, and migration pattern changes.

During the summer months, the main factor driving a southward breach migration is onshore waves. Once the precipitation becomes negligible, the river discharge plays a much lower role. Even though the river discharge remains relatively high for WY 2023 (10 m^3/s transitioning to 0.2 m^3/s for d_r and 4.5 m transitioning to 3.6 m h_r) compared to WY 2022 (0.01 m^3/s going to 0.005 m^3/s for d_r and 3.3 m going to 3.2 m h_r). These values are within the normal averages for both years. Values of S_{xy} for both years are predominantly negative indicating the onshore wave radiation stress is southward on Pajaro beach. This is interesting considering the observed wave direction for the summer months for both years has large weekly swings north and south of shore normal as discussed previously. Despite this fact, S_{xy} remains negative. In addition to the large directional wave swings, the overall H_r minimizes and stabilizes for both years. With the river unable to counteract the constant negative S_{xy}, the breach has a steady migration northward for WY 2022 and WY2023. This indicates that during the summer months, the Pajaro river breach migration is wave dominated.

E. MISSING COMPARISON VARIABLE: BREACH DEPTH

The depth of the Pajaro lagoon and the Pajaro River breach depths were not measured during this study, however, it is believed that this may play a key role in predicting breach migration, breach opening, and breach closure. As discussed previously, WY 2023 was unusual compared to WY 2022 and the previous years before due to the shear amount of rainwater outflow that Pajaro had that led to massive discharge rates and likely caused considerable sediment to be deposited offshore. This inherently makes the lagoon and the breach much deeper during the winter months of WY 2023 than in the past. The river breach never closed upon its initial opening and remained open past the end of the water year. This behavior is not common for this beach as can be observed from the previous year where three closures were observed. Although not directly measured, one could easily conclude that the breach was much deeper toward the end of WY 2023 making

the process of onshore sediment deposition brought on by the wave driven coast to take much longer than in previous years.

THIS PAGE INTENTIONALLY LEFT BLANK

VI. CONCLUSION

In this study, three hypotheses were presented: a) high river discharge enhances inlet migration and longer breach times, b) annual breach time periods for a normal (or dry) year is from November to September but longer for wetter years, and c) wave direction plays a critical role in net seasonal migration.

With regards to hypothesis a), this study has shown that high river discharge during unusually rainy years correlates strongly to increased overall southerly breach migration for the Pajaro river estuary when compared to normal rainfall years. Additionally, during high discharge periods, the winter months migration is more sporadic (large swings between northerly and southerly breach migration) as can be seen in Figures 18 and 19 respectively.

For hypothesis b), WY 2022 followed the standard annual migration period by opening at the end of October 2021 and closing in September 2022. WY 2023, did start at the predicted time (initial breach in November 2022), but remained open past the end of the water year. The river discharge rates were much higher and remained high (when compared to 2022) well into the beginning of April 2022. This drastic and prolonged increase in river discharge directly correlates to the breach remaining open past the end of the heavy rainfall water year.

Finally for hypothesis c), the primary river breach forcing mechanisms are H_s, wave direction, river discharge rate (d_r), and river height (h_r). All these forcing mechanisms play a critical role in driving breach migration as has been shown. During the winter (wet) months, breach migration is driven by d_r and h_r. Once the rain ceases and the transition into the summer (dry) months occurs, the breach migration is driven by H_s and wave direction. This data strongly correlates to a previous study that had similar results when comparing the driving factors for inlet migration (Behrens et al. 2009). Behrens (2009) showed that high river discharge and high wave events both are driving factors when it comes to inlet migration at ephemeral rivers.

Future work could include calculating the depth of the river breach throughout the year. It is believed that the depth of the river breach plays a large part in determining how long the river will stay breached as it would take longer for offshore sediment to fill the gaps. This information would greatly enhance the results found in this report. Additionally, using LiDAR to capture and track the beach sediment transport on and offshore would further enhance the findings from this research by quantitatively showing where beach sediment is being transported and at what times. Finally, a longer study (multiple years with varying El Nino/La Nina seasons) of this area could show the potential impacts of ENSO cycles which could directly affect the forcing mechanisms that drive river migration.

APPENDIX

Date	Longshore (m) (North Pt)	Rate of Change (m/day)	Data Source
15-Dec-21	365.898	N/A	Walking Survey, Sentinel (L2A)
28-Jan-22	443.154	1.756	Walking Survey, Sentinel (L2A)
18-Feb-22	397.326	-2.182	Walking Survey, CIRN Image
11-Mar-22	346.765	-2.408	Walking Survey, Sentinel (L2A), CIRN Image
4-Apr-22	426.527	3.323	Sentinel (L2A)
29-Apr-22	418.857	-0.307	Sentinel (L2A)
06-10May 22	x	x	x
14-May-22	411.82	-0.469	Sentinel (L2A)
29-May-22	399.709	-0.807	Sentinel (L2A)
18-Jun-22	496.117	4.82	Sentinel (L2A)
3-Jul-22	517.803	1.446	Sentinel (L2A)
15-Jul-22	526.749	1.135	Walking Survey, Sentinel (L2A)
2-Aug-22	544.601	0.991	Sentinel (L2A)
24-Aug-22	562.571	0.896	Walking Survey, Sentinel (L2A)
16-Sep-22	587.954	1.103	Sentinel (L2A)
30-Sep-22	x	x	Walking Survey
25-Nov-22	x	x	N/A
14-Dec-22	478.39	x	Walking Survey
6-Jan-23	536.87	2.543	Walking Survey
20-Jan-23	630.171	6.664	Walking Survey

Date	**Longshore (m) (North Pt)**	**Rate of Change (m/day)**	**Data Source**
30-Jan-23	619.243	-1.093	Walking Survey
3-Mar-23	626.112	0.215	Walking Survey
21-Apr-23	601.337	-0.506	Walking Survey
24-Apr-23	695.594	31.419	Sentinel (L2A)
20-Jun-23	1010.84	5.531	Walking Survey, LiDAR
28-Jul-23	889.85	-3.184	Walking Survey, Sentinel
22-Aug-23	1103.41	8.542	Walking Survey, Sentinel
6-Sep-23	1154.53	3.408	Walking Survey, Sentinel
21-Sep-23	1249.97	6.363	Sentinel (L2A)
26-Sep-23	777.755	-94.443	Sentinel (L2A)

LIST OF REFERENCES

Barker, J. (Rusty), 2022: *Pajaro River Mouth 2021–2022 Monitoring*. Flood Control and Water Conservation District – Zone 7.

Behrens, D. K., F. A. Bombardelli, J. L. Largier, and E. Twohy, 2009: Characterization of time and spatial scales of a migrating rivermouth. *Geophys. Res. Lett.*, **36**, L09402, https://doi.org/10.1029/2008GL037025.

Bijoor, N., 2019: Pajaro River Watershed IRWM Plan. *Pajaro River Watershed Integrated Regional Water Management (IRWM) Factsheet*. https://www.pajaroriverwatershed.org/projects/irwmp.

Booysen, Z., and A. K. Theron, 2020: Methods for predicting berm height at temporarily open/closed estuaries. *Estuarine, Coastal and Shelf Science*, **245**, 106906, https://doi.org/10.1016/j.ecss.2020.106906.

Casella, E., J. Drechsel, C. Winter, M. Benninghoff, and A. Rovere, 2020: Accuracy of sand beach topography surveying by drones and photogrammetry. *Geo-Mar Lett*, **40**, 255–268, https://doi.org/10.1007/s00367-020-00638-8.

Colomina, I., and P. Molina, 2014: Unmanned aerial systems for photogrammetry and remote sensing: A review. *ISPRS Journal of Photogrammetry and Remote Sensing*, **92**, 79–97, https://doi.org/10.1016/j.isprsjprs.2014.02.013.

The County of Santa Cruz, 01OCT2021-30SEP2023: Corralitos Raws (COR) (CA22D628).

Davidson, M. A., B. D. Morris, and I. L. Turner, 2009: A simple numerical model for inlet sedimentation at intermittently open–closed coastal lagoons. *Continental Shelf Research*, **29**, 1975–1982, https://doi.org/10.1016/j.csr.2008.10.005.

Dawson, J., M. M. Orescanin, R. Clark, and K. O'Connor, 2023: Spatiotemporal variability of dissolved oxygen in response to morphological state in a central California coast bar-built estuary. *Estuarine, Coastal and Shelf Science*, **282**, 108241, https://doi.org/10.1016/j.ecss.2023.108241.

Dean, R. G., and R. A. Dalrymple, 2002: *Coastal Processes with Engineering Applications*. 1st ed. The Press Syndicate of the University of Cambridge, 475 pp.

Douglass, S. L., 1992: Estimating extreme values of run-up on beaches. *Journal of Waterway, Port, Coastal, and Ocean Engineering*, **118**, 220–224.

Fitzgerald, D. M., D. K. Hubbard, and D. Nummedal, 1978: Shoreline changes associated with tidal inlets along the South Carolina coast. *Coastal Zone '78, Symposium on Technical, Environmental, Socioeconomic, and Regulatory Aspects of C.Z.M.*, 1973–1994.

Holland, K. T., B. Raubenheimer, R. T. Guza, and R. A. Holman, 1995: Runup kinematics on a natural beach. *J. Geophys. Res.*, **100**, 4985–4993, https://doi.org/10.1029/94JC02664.

Jimenez, 2023: Pajaro River levee breaches, resulting in a chaotic emergency for thousands of displaced residents. *Monterey County Weekly*. https://www.montereycountyweekly.com/news/local_news/pajaro-river-levee-breaches-resulting-in-a-chaotic-emergency-for-thousands-of-displaced-residents/article_80a17e10-c35b-11ed-b68a-3b31a5e44d0d.html (Accessed October 24, 2023).

Kraus, N. C., A. Militello, and G. Todoroff, 2002: Barrier breaching processes and barrier spit breach, Stone Lagoon, California. *Shore & Beach*, **70**, 21.

——, K. Patsch, and S. Munger, 2008: Barrier beach breaching from the lagoon side, with reference to Northern California. *Shore & Beach*, **76**, 11.

McSweeney, S. L., D. M. Kennedy, I. D. Rutherfurd, and J. C. Stout, 2017: Intermittently Closed/Open Lakes and Lagoons: Their global distribution and boundary conditions. *Geomorphology*, **292**, 142–152, https://doi.org/10.1016/j.geomorph.2017.04.022.

Orescanin, M. M., and J. Scooler, 2018: Observations of episodic breaching and closure at an ephemeral river. *Continental Shelf Research*, **166**, 77–82, https://doi.org/10.1016/j.csr.2018.07.003.

Orescanin, M. M., W. Young, J. Coughlin, D. W. Herrmann, and J. Metcalf, 2019: Seasonal morphological change at a bar built estuary: Carmel River, CA. *Coastal Sediments 2019*, International Conference on Coastal Sediments 2019, Tampa/St. Petersburg, Florida, USA, World Scientific, 674–683.

Orescanin, M. M., J. Coughlin, and W. R. Young, 2021: Morphological response of variable river discharge and wave forcing at a bar-built estuary. *Estuarine, Coastal and Shelf Science*, **258**, 107438, https://doi.org/10.1016/j.ecss.2021.107438.

Plant, J. T., 2022: *UAS Analysis Of Wave Runup At Coastal California Ephemeral Rivers*. Master's thesis, Naval Postgraduate School, Monterey, CA.

Ranasinghe, R., and C. Pattiaratchi, 2003: The seasonal closure of tidal inlets: Causes and effects. *Coastal Engineering Journal*, **45**, 601–627, https://doi.org/10.1142/S0578563403000919.

Rich, A., and E. A. Keller, 2013: A hydrologic and geomorphic model of estuary breaching and closure. *Geomorphology*, **191**, 64–74, https://doi.org/10.1016/j.geomorph.2013.03.003.

Tung, T. T., D.-J. R. Walstrafoo, J. van de Graafff, and M. J. F. Stivef, 2009: Morphological modeling of tidal inlet migration and closure. *Journal of Coastal Research*, Proceedings of the 10th International Coastal Symposium ICS 2009, 1080–1084.

Wainwright, D. J., and T. E. Baldock, 2015: Measurement and modelling of an artificial coastal lagoon breach. *Coastal Engineering*, **101**, 1–16, https://doi.org/10.1016/j.coastaleng.2015.04.002.

Whitfield, A. K., M. Elliott, A. Basset, S. J. M. Blaber, and R. J. West, 2012: Paradigms in estuarine ecology – A review of the Remane diagram with a suggested revised model for estuaries. *Estuarine, Coastal and Shelf Science*, **97**, 78–90, https://doi.org/10.1016/j.ecss.2011.11.026.

THIS PAGE INTENTIONALLY LEFT BLANK

INITIAL DISTRIBUTION LIST

1. Defense Technical Information Center
   Fort Belvoir, Virginia

2. Dudley Knox Library
   Naval Postgraduate School
   Monterey, California